

Minimum-jerk velocity planning for mobile robot applications

Corrado Guarino Lo Bianco, *Member*

Abstract—The paper studies an assigned-time velocity planning problem for robotic systems that are subject to velocity and acceleration constraints. The planning problem, that is justified by several robotic applications, poses feasibility issues that are investigated in the paper. In particular, the paper shows that feasible solutions exist if and only if proper interpolating conditions are assigned, and proposes an efficient planning strategy, that is suitable for online implementations. Available degrees of freedom are used to smooth the velocity function by minimizing its maximum jerk.

I. INTRODUCTION

The optimal trajectory planning problem has been widely investigated in robotics. Several optimality criteria have been considered, but two of them are the most frequently adopted: Traveling times are commonly minimized for productivity reasons, while minimum-jerk trajectories are planned for smoothness reasons.

Minimum-time trajectories have been initially handled by means of offline constrained optimization approaches. In particular, constraints typically concerned kinematics bounds – joint velocities, accelerations, and jerks cannot evidently exceed some given maximum values [1] – and/or dynamics bounds – joint torques [2], [3] or torque derivatives [4] must be limited within given intervals. – In order to handle rapidly mutating scenarios, recent approaches focus on online strategies. In [5], for example, step reference signals are interpolated by trajectories that admit bounded velocities, accelerations, and jerks. A similar result is achieved in [6] by using a parabolic shape for the jerk signal, thus obtaining almost optimal solutions, while the exact solution that has been proposed in [7] is also able to manage variable input signals. The study on minimum-time solutions has been recently enlarged in [8]–[11] by considering multidimensional trajectories.

The generation of minimum-jerk trajectories, that are typically used to reduce mechanical solicitations and to obtain better control performances, represents another optimal planning problem that is often considered in the literature. Traveling time is not minimized, but, conversely, it is determined by the task. Minimum-jerk fixed-time trajectories can easily be applied in robotic or electromechanical contexts, where they are used to avoid collisions [12] or to intercept moving objects [13]. It is also worth to mention the existence of hybrid strategies, like the one that is proposed in [14] for a multi-axis system, in which the performance index is obtained by combining traveling time with the integral of the squared jerk along the curve.

The minimum-jerk problem was introduced in [15] for a multidimensional point-to-point movement subject to torque constraints. The problem was offline solved by means of standard optimization programs. A global approach, that was based on interval techniques, was later proposed in [16] for an unconstrained point-to-point movement.

Even in this field, the attention is currently migrating to online strategies. Still considering unconstrained problems and point-to-point movements, in [17] and in [12], online approaches have been proposed for the minimization of the integral of the squared jerk. Alternatively, a genetic algorithm has been used in [18] in order

This work was partially supported by the Ateneo Italo Tedesco in the framework of a Vigoni project.

© 2013 IEEE. Personal use of this material is permitted. Permission from IEEE must be obtained for all other uses, in any current or future media, including reprinting/republishing this material for advertising or promotional purposes, creating new collective works, for resale or redistribution to servers or lists, or reuse of any copyrighted component of this work in other works.

to manage a larger class of problems, by considering constraints on positions, velocities, and accelerations and by admitting generic interpolating conditions.

The constrained minimum-jerk problem that was studied in [18], differently from minimum-time problems or from minimum-jerk unconstrained problems, is characterized by feasibility issues: Depending on the interpolating conditions and on the constraints, it can admit no feasible solutions. An initial study on the feasibility issues of minimum-jerk problems was proposed in [13] by only considering the velocity constraint. The analysis was deepened in [19] by introducing the acceleration bounds and by providing sufficient conditions for the solution existence.

In this paper, the feasibility problem is further analyzed and necessary and sufficient conditions are devised to check the existence of solutions. Additionally, if such conditions are satisfied, a procedure, that is exclusively based on closed form expressions, is proposed for an efficient evaluation of an initial feasible trajectory. Such trajectory is subsequently improved by means of an optimization algorithm that minimizes its maximum jerk by acting over a suitably parametrized subset of the complete set of feasible solutions. The knowledge of an initial feasible solution is mandatory, because the problem is nonlinear: Offline commercial programs are often unable to find the feasible area. The results here proposed were early anticipated, without demonstrations, in [20]. In this new paper, the approach is analytically demonstrated and more experimental results are reported in order to verify its performances.

The paper is organized as follows. The problem motivations are discussed in §II, where the velocity planning problem is also formulated. In subsequent §III, necessary and sufficient conditions are proposed to guarantee the existence of feasible solutions, while in §IV a procedure is devised for the evaluation of one of them: Its feasibility is proved in the Appendix section. In §V, the reliability of the algorithm is checked by means of an extended set of tests. Final considerations are drawn in §VI.

II. THE VELOCITY PLANNING PROBLEM: MOTIVATION AND REQUIREMENTS

The minimum-jerk problem considered in this paper was originally motivated by the planning scenario that is shown in Fig. 1. A mobile robot, that is placed at time $t = 0$ in B , must hit a ball initially located in A . A supervisor, on the basis of the ball trajectory, poses the interception point in C at time $t = t_e$. Clearly, for a correct task accomplishment, the fulfillment of the assigned traveling time is mandatory. The desired motion can be achieved, e.g., by means of the control strategy proposed in [21], that uses the path-velocity decomposition paradigm [22], i.e., the trajectory is obtained by combining a parametric path $f(s)$, with a longitudinal time-law $s(t)$. The path can be evaluated, e.g., according to the procedure proposed in [23], while $s(t)$ can be computed according to the minimum-jerk strategy described in this paper.

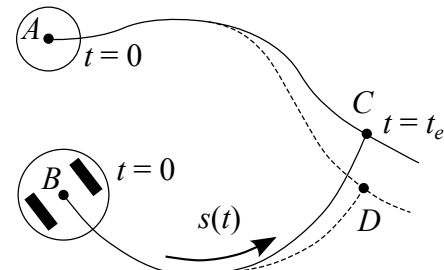


Fig. 1. Trajectory planning for a mobile robot.

Mentioned application directly suggests the time-law planning requirements. Function $s(t)$ must guarantee that path length s_e is exactly traversed in t_e seconds, i.e., $s(t_e) = s_e$. As a consequence, velocity $v(t) := \dot{s}(t)$ must fulfill the following equation

$$s_e = \int_0^{t_e} v(\tau) d\tau. \quad (1)$$

Because of the analysis that was reported in [21], $v(t)$, for smoothness reasons, must be continuous together with its first derivative, i.e., $v(t) \in \mathcal{C}^1([0, t_e])$. Still for smoothness reasons, the longitudinal jerk along the trajectory must be minimized.

The robot physical limits must be necessarily fulfilled. This result is achieved by limiting $v(t)$ and $a(t)$ within proper bounds

$$0 < v(t) \leq \tilde{v}, \forall t \in (0, t_e), \quad (2)$$

$$|a(t)| \leq \tilde{a}, \forall t \in [0, t_e], \quad (3)$$

where \tilde{v} and \tilde{a} are user defined limits. It is worth noticing that the velocity lower bound has been posed equal to zero in order to avoid useless backward movements.

The \mathcal{C}^1 -continuity of $v(t)$ must also be guaranteed in case of anticipated re-plannings, e.g., to reach the new contact point D in Fig. 1. To this purpose, velocity $v(0)$ and acceleration $a(0)$ need to be arbitrarily assigned. Analogously, the target is reached with the correct status of motion only if proper values can be imposed to $v(t_e)$ and to $a(t_e)$. Thus, named v_s and a_s the boundary conditions at the start point, and v_e and a_e those at the end point, the following equations must be satisfied

$$v(0) = v_s, v(t_e) = v_e, a(0) = a_s, a(t_e) = a_e. \quad (4)$$

As it has been early announced, only positive velocities are considered: A velocity equal to zero is only admitted for $t = 0$ and $t = t_e$, so that $v_s, v_e \in [0, \tilde{v}]$. Moreover, when $v_s = 0$, condition (2) is satisfied only if $a_s \geq 0$, while, if $v_e = 0$, it is necessary to impose $a_e \leq 0$. Analogously, if $v_s = \tilde{v}$, it is necessary to guarantee that $a_s \leq 0$, while if $v_e = \tilde{v}$ then, necessarily, $a_e \geq 0$. Finally, the boundary conditions on the acceleration must also satisfy (3), i.e., $a_s, a_e \in [-\tilde{a}, \tilde{a}]$.

Due to previous definitions and assignments, it is possible to define a feasible profile $v(t)$ as follows

Definition 1: A curve $v(t) \in \mathcal{C}^1([0, t_e])$ is *feasible* if it satisfies conditions (1)–(4).

The paper is devoted to solve the following planning problem

Problem 1: Given a path of length s_e and a traveling time t_e , let design a feasible velocity function $v(t) \in \mathcal{C}^1([0, t_e])$ that satisfies generic boundary conditions $v_s, v_e \in [0, \tilde{v}]$ and $a_s, a_e \in [-\tilde{a}, \tilde{a}]$, where $\tilde{v}, \tilde{a} > 0$ are assigned and proper bounds on the velocity and on the acceleration.

The problem is characterized by feasibility issues. For this reason, necessary and sufficient closed form expressions must be devised in order to verify the existence of a solution. This is an important feature since, if *Problem 1* is unfeasible, the supervisor must immediately try a different approach to the moving object.

An important aspect that must be carefully considered is represented by the evaluation times. For the robotic application here considered, good performances are obtained if trajectories are updated every 1e-1 s: The computational burden of the time-law planner must be compatible with such time. Actually, as shown in §V, obtained evaluation times are well below such limit, thus the proposed approach can also be used in more demanding contexts.

In the paper, \tilde{v} and \tilde{a} are supposed to be constant while, in more realistic scenarios, they are influenced by kinematic and/or dynamic constraints. For variable values of \tilde{v} and \tilde{a} , the feasibility conditions provided in the following are only sufficient to prove the

solutions existence, but the planning scheme is still usable, as proved, e.g., in [24], where the time-law was found by considering variable constraints that were function of the path geometry.

III. A FEASIBILITY RESULT

The posed feasibility issue is solved by the following proposition:

Proposition 1: A feasible solution of *Problem 1* exists with certainty if and only if the following conditions simultaneously hold

$$|v_s - v_e| < \tilde{a}t_e, \quad (5)$$

$$\begin{cases} s_e < \left[t_e + \frac{v_s + v_e - \tilde{v}}{\tilde{a}} \right] \tilde{v} - \frac{v_s^2 + v_e^2}{2\tilde{a}} & \text{if } v_s + v_e + \tilde{a}t_e > 2\tilde{v} \\ s_e < \frac{(v_s + v_e)t_e}{2} + \frac{\tilde{a}t_e^2}{4} - \frac{(v_s - v_e)^2}{4\tilde{a}} & \text{if } v_s + v_e + \tilde{a}t_e \leq 2\tilde{v} \end{cases} \quad (6)$$

$$\begin{cases} s_e > \frac{v_s^2 + v_e^2}{2\tilde{a}} & \text{if } v_s + v_e - \tilde{a}t_e < 0 \\ s_e > \frac{(v_s + v_e)t_e}{2} - \frac{\tilde{a}t_e^2}{4} + \frac{(v_s - v_e)^2}{4\tilde{a}} & \text{if } v_s + v_e - \tilde{a}t_e \geq 0 \end{cases} \quad (7)$$

Proof - The proof is based on the hypothesis that assigned interpolating conditions are compatible with the bounds on the maximum velocity and acceleration, i.e., $v_s, v_e \in [0, \tilde{v}]$, $a_s, a_e \in [-\tilde{a}, \tilde{a}]$.

Necessity - It is necessary to prove that, for any feasible solution of *Problem 1*, conditions (5)–(7) hold.

Velocity $v(t)$ can be expressed as

$$v(t) = v_s + \int_0^t a(\tau) d\tau. \quad (8)$$

If $v(t)$ is feasible, then condition (3) holds, so that it is possible to infer that

$$v(t) \leq v_s + \int_0^t \tilde{a} d\tau = v_s + \tilde{a}t, \quad \forall t \in [0, t_e], \quad (9)$$

$$v(t) \geq v_s - \int_0^t \tilde{a} d\tau = v_s - \tilde{a}t, \quad \forall t \in [0, t_e]. \quad (10)$$

Both conditions must also apply for $t = t_e$. Thus, it is possible to assert that, for any feasible solution, the following two inequalities must simultaneously apply

$$v_e = v(t_e) \leq v_s + \tilde{a}t_e, \quad (11)$$

$$v_e = v(t_e) \geq v_s - \tilde{a}t_e. \quad (12)$$

Simple manipulations on (11) and (12) lead to the following inequality

$$|v_s - v_e| \leq \tilde{a}t_e. \quad (13)$$

In (13), the equality sign is only compatible with a solution in which $v(t)$ is a linear segment directly joining v_s with v_e and characterized by the following interpolating conditions: $a_s = a_e = (v_e - v_s)/t_e$, $|a_s| = |a_e| = \tilde{a}$, $s_e = (v_s + v_e)t_e/2$. This particular case can be handled separately while, for generic interpolating condition, (5) must be used instead of (13).

The same result could also have been achieved by evaluating $v(t)$ through a backward integration, i.e., by starting from $t = t_e$

$$v(t) = v_e + \int_{t_e}^t a(\tau) d\tau. \quad (14)$$

Thus, any feasible profile must also fulfill the following inequalities

$$v(t) \leq v_e - \int_{t_e}^t \tilde{a} d\tau = v_e + \tilde{a}(t_e - t), \quad \forall t \in [0, t_e], \quad (15)$$

$$v(t) \geq v_e + \int_{t_e}^t \tilde{a} d\tau = v_e - \tilde{a}(t_e - t), \quad \forall t \in [0, t_e]. \quad (16)$$

A few algebraic manipulations lead again to (13) and, in turn, to (5).

Equations (9), (10), (15), and (16) are also instrumental in order to devise (6) and (7). Evidently, (9), (10), (15), and (16) map the

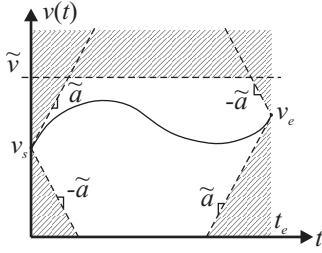


Fig. 2. An example of the feasible area for a generic velocity profile.

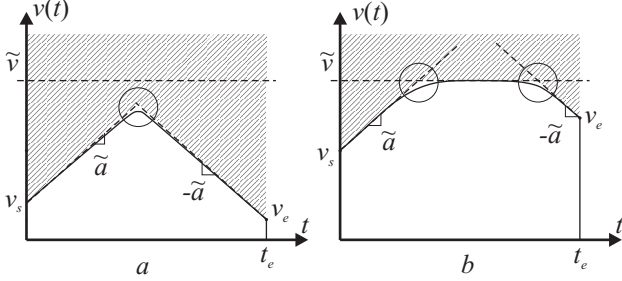


Fig. 3. Maximum admissible area of any feasible velocity profile.

acceleration bounds into equivalent bounds for the velocity profile. Further constraints on $v(t)$ are added by (2), thus it is possible to assert that any feasible profile must lay inside the white area that is shown in Fig. 2. This implies that the area of any feasible curve $v(t)$ is superiorly and inferiorly bounded because of the constraints. In particular, (6) and (7) respectively account for the limits on the maximum and on the minimum area that any feasible $v(t)$ can assume depending on the interpolating conditions.

Let us focus the attention on (6). Depending on the initial and final boundary conditions, the two situations that are shown in Fig. 3 can arise. In the case of Fig. 3a, the velocity upper bound \tilde{v} can never be reached owing to \tilde{a} , v_s and v_e . By means of some algebraic manipulations it is possible to prove that the configuration of Fig. 3a is characterized by $v_s + v_e + \tilde{a}t_e \leq 2\tilde{v}$ while, viceversa, the configuration of Fig. 3b is characterized by $v_s + v_e + \tilde{a}t_e > 2\tilde{v}$. As a consequence, the maximum admissible area of any feasible velocity function cannot be greater than the two white areas of Fig. 3. It is simple to prove that the area of the feasible zone in Fig. 3a is equal to $\frac{(v_s + v_e)t_e}{2} + \frac{\tilde{a}t_e^2}{4} - \frac{(v_s - v_e)^2}{4\tilde{a}}$, while, in the case of Fig. 3b, it is equal to $\left[t_e + \frac{v_s + v_e - \tilde{v}}{\tilde{a}} \right] \tilde{v} - \frac{v_s^2 + v_e^2}{2\tilde{a}}$. In both the two cases, such maximum values can never be exactly reached by means of a feasible curve: Because of the required \mathcal{C}^1 continuity, it is not possible to generate cuspid points like those pointed out by the circles of Fig. 3, so that, according to (6), for any feasible solution, s_e is strictly smaller than the above mentioned limits.

Similar considerations apply for (7), but the bounds concern the minimum admissible area of any feasible curve. One of the two cases that are shown in Fig. 4a or in Fig. 4b can appear. In the first case $v_s + v_e - \tilde{a}t_e > 0$ and the area of $v(t)$ must be greater than $\frac{(v_s + v_e)t_e}{2} - \frac{\tilde{a}t_e^2}{4} + \frac{(v_s - v_e)^2}{4\tilde{a}}$, while in the second one $v_s + v_e - \tilde{a}t_e \geq 0$ and s_e must be greater than $\frac{v_s^2 + v_e^2}{2\tilde{a}}$. Again, the two given limits cannot be exactly obtained owing to the continuity constraint.

Sufficiency - The sufficiency condition is proved if it is possible to demonstrate that (5)–(7) imply that a feasible solution for *Problem 1* exists with certainty. In the next §IV a method for the synthesis of a feasible solution is proposed under the hypothesis that (5)–(7)

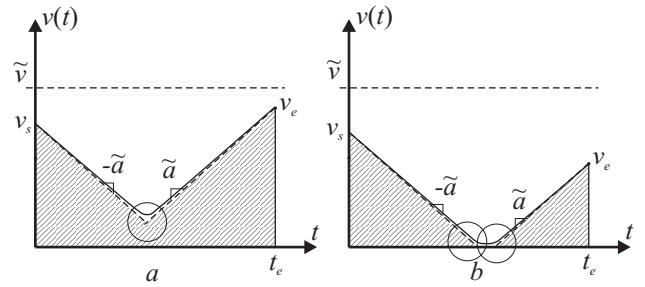


Fig. 4. Minimum admissible area of any feasible velocity profile.

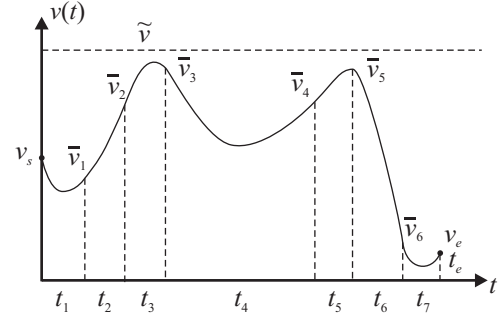


Fig. 5. Velocity function $v(t)$.

simultaneously hold. ■

IV. A FEASIBLE SOLUTION

Every time conditions (5)–(7) are fulfilled, it is possible to devise a feasible solution for *Problem 1*. Such solution is not unique, so that the approach that is proposed in the following returns just one among all the feasible functions. The proposed solution has two peculiarities. First of all, it is obtained by means of closed form expressions, thus with a negligible evaluation time. Secondly, due to the adopted parametrization, it is characterized by several degrees of freedom that can be later used to optimize a given performance index. Since in this paper smoothness covers a relevant role, available degrees of freedom are spent to minimize the maximum jerk associated to $v(t)$.

The adopted velocity function $v(t)$ is made of seven parabolic curves that are defined over as many time intervals t_i ($i = 1, \dots, 7$)

$$v_i(t) := p_{1i} + 2p_{2i}t + 3p_{3i}t^2, \quad t \in [0, t_i]. \quad (17)$$

Correspondingly, for each $v_i(t)$ it is possible to define a curvilinear coordinate $s_i(t)$, an acceleration function $a_i(t)$, and a jerk function $j_i(t)$ where

$$s_i(t) = p_{1i}t + p_{2i}t^2 + p_{3i}t^3, \quad t \in [0, t_i], \quad (18)$$

$$a_i(t) = 2p_{2i} + 6p_{3i}t, \quad t \in [0, t_i], \quad (19)$$

$$j_i(t) = 6p_{3i}, \quad t \in [0, t_i]. \quad (20)$$

Notice that, at the beginning of each interval, time t and curvilinear coordinate $s_i(t)$ start from zero. Boundary velocities and accelerations are synthetically indicated in the following by “overlined” symbols, so that, e.g., $v_2(0) = v_1(t_1) = \bar{v}_1$ (see also Fig. 5).

The choice of a seven segments profile guarantees that a feasible solution can be found independently from the assigned planning conditions. The most critical situations are those in which (6) or (7) are almost violated. In such cases, the admissible solutions must necessarily assume shapes that are similar to those that are shown in Figs. 3b and 4b, i.e., they are given by linear segments, that must be properly joined in order to fulfill the continuity condition on the acceleration signal: With a seven segments profile, like the one

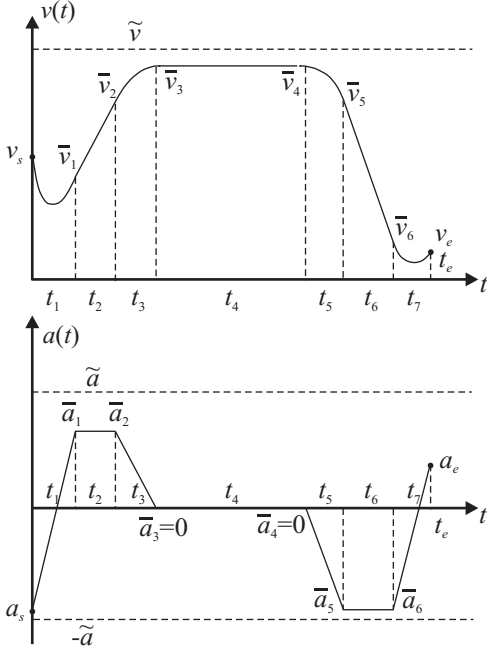


Fig. 6. Typical velocity and acceleration profiles obtained at the end of *Step 1*.

that is shown in Fig. 6, it is always possible to generate a feasible solution. Profiles with a higher number of segments can be evidently adopted, but this choice would obviously increase the evaluation times of the subsequent optimization problem. Similar considerations hold for the degree of the polynomial curves: The seven segments, cubic polynomial profile is the minimum order solution that can be used to interpolate any free set of planing data and that leaves sufficient degrees of freedom for the jerk minimization.

Coefficients p_{ji} can be evaluated according to the equations that are provided in [20]. They were originally obtained by imposing the \mathcal{C}^1 continuity of the overall curve and the fulfillment of boundary conditions (4). Coefficients p_{ji} are parametrized by seven traveling times, i.e., $t_1, t_2, t_3, t_4, t_5, t_6, t_7$, seven velocities, i.e., $\bar{v}_0, \bar{v}_1, \bar{v}_2, \bar{v}_3, \bar{v}_4, \bar{v}_5, \bar{v}_7$, and two accelerations, i.e., \bar{a}_0, \bar{a}_7 . Some of those parameters are imposed by the problem constraints. For example, the constraint on the total traveling time is taken into account by imposing

$$t_4 = t_e - \sum_{i=1,2,3,5,6,7} t_i. \quad (21)$$

Analogously, terms $\bar{v}_0 = v_s$, $\bar{a}_0 = a_s$, $\bar{v}_7 = v_e$, and $\bar{a}_7 = a_e$ are assigned by the user, so that the overall profile is actually function of the following eleven free elements

$$\begin{aligned} \mathbf{h} &= [h_1 \ h_2 \ h_3 \ h_4 \ h_5 \ h_6 \ h_7 \ h_8 \ h_9 \ h_{10} \ h_{11}]^T \\ &:= [t_1 \ t_2 \ t_3 \ t_5 \ t_6 \ t_7 \ \bar{v}_1 \ \bar{v}_2 \ \bar{v}_3 \ \bar{v}_4 \ \bar{v}_5]^T, \end{aligned} \quad (22)$$

where $\mathbf{h} \in \mathcal{H} := (0, t_e)^6 \times (0, \bar{v})^5$.

Let us suppose that (5)–(7) simultaneously hold and that conditions $v_s, v_e \in [0, \bar{v}]$, and $a_s, a_e \in [-\bar{a}, \bar{a}]$ are fulfilled. Moreover, let us indicate by S the area of $v(t)$. Under such hypotheses, it is possible to evaluate a feasible solution for *Problem 1* by means of following four steps procedure:

Step 1 - Specialize the spline equations in order to obtain an appropriate shape for $v(t)$;

Step 2 - Find a velocity profile such that $v(t) \in [0, \bar{v}]$, $a(t) \in [-\bar{a}, \bar{a}]$, traveling time is equal to t_e and $S > s_e$;

Step 3 - Find a velocity profile such that $v(t) \in [0, \bar{v}]$, $a(t) \in [-\bar{a}, \bar{a}]$, traveling time is equal to t_e and $S < s_e$;

Step 4 - Find a feasible $v(t)$.

The four steps procedure is detailed in the following, while, in order to lighten the presentation, the feasibility of $v(t)$ is proved in the Appendix section.

Step 1 - The spline equations are specialized in order to obtain the almost trapezoidal shape of $v(t)$ that is shown in Fig. 6. In particular, this result is obtained by imposing the linearity of $v(t)$ inside intervals 2, 4, and 6 ($p_{32} = p_{34} = p_{36} = 0$), the condition $\bar{v}_4 = \bar{v}_3$, and by assigning $t_3 = t_5 = t_7 := t_1$. The simplified profile, which coefficients are reported in [20], is parametrized by means of a reduced number of coefficients, more precisely it is only function of t_1, t_2, t_6 , and v_3 .

The velocity profile is further specialized by choosing the maximum strictly positive value of t_1 that simultaneously satisfies the following conditions

$$t_1 \leq \begin{cases} \frac{t_e}{4} & \text{if } (v_s = 0) \& (v_e = 0) \\ \min \left\{ \frac{2v_e}{a_e + 2a_s + 2\bar{a}}, \frac{2(-t_e \bar{a} + v_e)}{a_e + 2a_s - 6\bar{a}} \right\} & \text{if } (v_s = 0) \& (v_e > 0) \\ \min \left\{ -\frac{2v_s}{a_s + 2a_e - 2\bar{a}}, \frac{2(t_e \bar{a} - v_s)}{a_s + 2a_e + 6\bar{a}} \right\} & \text{if } (v_s > 0) \& (v_e = 0) \\ \min \left\{ \frac{2(v_s + v_e - t_e \bar{a})}{a_e - a_s - 4\bar{a}}, \frac{2v_s}{2\bar{a} - a_s}, \frac{2v_e}{2\bar{a} + a_e} \right\} & \text{if } (v_s > 0) \& (v_e > 0) \& (v_s + v_e - \bar{a}t_e < 0) \end{cases}, \quad (23)$$

$$t_1 \leq \begin{cases} \frac{t_e}{4} & \text{if } (v_s = \bar{v}) \& (v_e = \bar{v}) \\ \min \left\{ \frac{-2(-v_e + \bar{v})}{a_e + 2a_s - 2\bar{a}}, \frac{-2(\bar{v} - t_e \bar{a} - v_e)}{2a_s + 6\bar{a} + a_e} \right\} & \text{if } (v_s = \bar{v}) \& (v_e < \bar{v}) \\ \min \left\{ \frac{2(\bar{v} - v_s)}{2\bar{a} + a_s + 2\bar{a}}, \frac{2(-v_s - t_e \bar{a} + \bar{v})}{a_s - 6\bar{a} + 2a_e} \right\} & \text{if } (v_s < \bar{v}) \& (v_e = \bar{v}) \\ \min \left\{ \frac{2(v_e + v_s - 2\bar{v} + t_e \bar{a})}{4\bar{a} + a_e - a_s}, \frac{2(\bar{v} - v_s)}{2\bar{a} + a_s}, \frac{2(\bar{v} - v_e)}{2\bar{a} - a_e} \right\} & \text{if } (v_s < \bar{v}) \& (v_e < \bar{v}) \& (v_s + v_e + \bar{a}t_e) > 2\bar{v} \end{cases}, \quad (24)$$

$$t_1 \leq \min \left\{ \frac{2(v_s - v_e + t_e \bar{a})}{10\bar{a} - a_e - a_s}, \frac{2(v_e - v_s + t_e \bar{a})}{10\bar{a} + a_e + a_s} \right\} \quad \text{if } (v_s + v_e + \bar{a}t_e \leq 2\bar{v}) \quad \text{or} \quad (v_s + v_e - \bar{a}t_e \geq 0), \quad (25)$$

$$t_1 < \tilde{t}(\alpha, \beta, \delta), \quad (26)$$

$$t_1 < \hat{t}(\mu, \rho, v). \quad (27)$$

where $\min\{\cdot\}$ indicates the minimum value of a set, while $\tilde{t}(\alpha, \beta, \delta)$ and $\hat{t}(\mu, \rho, v)$ represent the minimum, strictly positive, root of equations $\alpha t^2 + \beta \tilde{t} + \delta = 0$ and $\mu t^2 + \rho \hat{t} + v = 0$, which coefficients are respectively defined in Table I.

In the Appendix section, it is shown that conditions (23)–(27) are essential in order to find a solution that fulfills (1) and (2), i.e., the area and the velocity constraints.

At the end of *Step 1* all the curve parameters have been assigned apart from partial traveling times t_2, t_6 , and velocity \bar{v}_3 .

Step 2 - A velocity function $v(t)$ is found such that $v(t) \in [0, \bar{v}]$, $a(t) \in [-\bar{a}, \bar{a}]$, and $S < s_e$. To this purpose, t_2, t_6 and \bar{v}_3 are selected as follows

$$\bar{v}'_3 = \begin{cases} a_s t_1 & \text{if } (v_s = 0) \& (v_e \geq 0) \\ -a_e t_1 & \text{if } (v_s > 0) \& (v_e = 0) \\ 0 & \text{if } (v_s > 0) \& (v_e > 0) \& (v_s + v_e - \bar{a}t_e < 0) \\ \frac{6\bar{a} + a_s - a_e}{4} t_1 + \frac{v_s + v_e - t_e \bar{a}}{2} & \text{if } (v_s > 0) \& (v_e > 0) \& (v_s + v_e - \bar{a}t_e \geq 0) \end{cases}, \quad (28)$$

$$t'_2 := \begin{cases} 0 & \text{if } v_s \leq \bar{v}'_3 \\ \frac{v_s - \bar{v}'_3}{\bar{a}} + \left(\frac{a_s}{2\bar{a}} - 1 \right) t_1 & \text{if } v_s > \bar{v}'_3 \end{cases}, \quad (29)$$

TABLE I
COEFFICIENTS THAT ARE USED FOR THE EVALUATION OF t_1

| | |
|---|---|
| $(v_s = 0) \& (v_e = 0)$ | $\alpha = -\frac{\frac{sa_s}{3}}{3} - \frac{ae}{3}$ $\beta = t_e a_s$ $\delta = -s_e$ |
| $(v_s = 0) \& (v_e > 0)$ | $\alpha = a_s \frac{a_s + a_e}{2\bar{a}} - \frac{14a_s + a_e}{12} + \frac{a_e^2}{8\bar{a}}$ $\beta = \frac{v_e + 2t_e a_s}{2} - v_e \frac{2a_s + a_e}{2\bar{a}}$ $\delta = \frac{v_e^2}{2\bar{a}} - s_e$ |
| $(v_s > 0) \& (v_e = 0)$ | $\alpha = a_e \frac{a_s + a_e}{2\bar{a}} + \frac{14a_e + a_s}{12} + \frac{a_s^2}{8\bar{a}}$ $\beta = \frac{v_s + 2t_e a_e}{2} + v_s \frac{2a_e + a_s}{2\bar{a}}$ $\delta = \frac{v_s^2}{2\bar{a}} - s_e$ |
| $(v_s > 0) \& (v_e > 0)$ $\& (v_s + v_e - \tilde{a}t_e < 0)$ | $\alpha = \frac{a_s - a_e}{12} + \frac{a_s^2 + a_e^2}{8\bar{a}}$ $\beta = \frac{a_s v_s - a_e v_e}{2\bar{a}} + \frac{v_s + v_e}{2}$ $\delta = \frac{v_s^2 + v_e^2}{2\bar{a}} - s_e$ |
| $(v_s > 0) \& (v_e > 0)$ $\& (v_s + v_e - \tilde{a}t_e \geq 0)$ | $\alpha = \frac{2(a_e - a_s) + 9\bar{a}}{12} + \frac{(a_s + a_e)^2}{16\bar{a}}$ $\beta = \frac{(a_s + a_e)(v_s - v_e)}{2(\bar{a} + a_s - a_e)} + \frac{4}{2(\bar{a} + a_s - a_e)t_e}$ $\delta = \frac{(v_s + v_e)4t_e}{2} - \frac{\tilde{a}t_e^2}{4} + \frac{(v_s - v_e)^2}{4a} - s_e$ $\mu = -\frac{sa_s}{3} - \frac{ae}{3}$ $\rho = t_e a_s$ $v = -s_e + \tilde{v}t_e$ |
| $(v_s = \tilde{v}) \& (v_e < \tilde{v})$ | $\mu = -a_s \frac{a_s + a_e}{2\bar{a}} - \frac{14a_s + a_e}{12} - \frac{a_e^2}{8\bar{a}}$ $\rho = \frac{v_e + 2t_e a_s}{2} + v_e \frac{2a_s + a_e}{2\bar{a}} - \frac{a_e^2 + 2a_s}{2\bar{a}} \tilde{v}$ $v = -\frac{v_e^2}{2\bar{a}} - \tilde{v} \frac{\tilde{v} - 2t_e \tilde{a} - 2t_e \tilde{a}}{2\bar{a}} - s_e$ |
| $(v_s < \tilde{v}) \& (v_e = \tilde{v})$ | $\mu = -a_e \frac{a_s + a_e}{2\bar{a}} + \frac{14a_e + a_s}{12} - \frac{a_s^2}{8\bar{a}}$ $\rho = \frac{v_s - 2t_e a_e}{2} - v_s \frac{2a_e + a_s}{2\bar{a}} - \tilde{v} \frac{a - 2a_e - a_s}{2\bar{a}}$ $v = -\frac{v_s^2}{2\bar{a}} - \tilde{v} \frac{\tilde{v} - 2v_s - 2t_e \tilde{a}}{2\bar{a}} - s_e$ |
| $(v_s < \tilde{v}) \& (v_e < \tilde{v})$ $\& (v_s + v_e + \tilde{a}t_e > 2\tilde{v})$ | $\mu = \frac{a_s - a_e}{12} - \frac{a_s^2 + a_e^2}{8\bar{a}}$ $\rho = \frac{(a_s - a_e)\tilde{v} - a_s v_s + a_e v_e + (v_e + v_s - 2\tilde{v})\tilde{a}}{2\bar{a}}$ $v = (t_e + \frac{v_s + v_e - \tilde{v}}{a})\tilde{v} - \frac{v_s^2 + v_e^2}{2\bar{a}} - s_e$ |
| $(v_s < \tilde{v}) \& (v_e < \tilde{v})$ $\& (v_s + v_e + \tilde{a}t_e \leq 2\tilde{v})$ | $\mu = \frac{2(a_e - a_s) - 9\bar{a}}{12} - \frac{(a_s + a_e)^2}{16\bar{a}}$ $\rho = \frac{(a_s + a_e)(v_e - v_s)}{4\bar{a}} + \frac{4}{(a_s - a_e - 2\tilde{a})t_e}$ $v = \frac{(v_s + v_e)4t_e}{2} + \frac{\tilde{a}t_e^2}{4} + \frac{(v_s - v_e)^2}{4\bar{a}} - s_e$ |

$$t'_6 := \begin{cases} 0 & \text{if } v_e \leq \bar{v}'_3 \\ \frac{v_e - \bar{v}'_3}{\tilde{a}} - \left(\frac{a_e}{2\tilde{a}} + 1 \right) t_1 & \text{if } v_e > \bar{v}'_3 \end{cases} . \quad (30)$$

It is worth to point out that the obtained solution is not feasible because it does not fulfill neither the area, nor the velocity constraints (indeed, $v(t)$ can be equal to zero inside $[0, t_e]$). Conversely, the acceleration constraint is certainly satisfied since, by means of few algebraic manipulations, it is possible to prove that $a_1(t_1) = -\tilde{a}$ and $a_7(0) = \tilde{a}$. $v(t)$ assumes a shape that is similar to one of those that are shown in Fig. 4.

Step 3 - A velocity function $v(t)$ is found such that $v(t) \in [0, \bar{v}]$, $a(t) \in [-\tilde{a}, \tilde{a}]$, and $S > s_e$. To this purpose, t_2, t_6 and \bar{v}_3 are selected according to the following equations

$$t_2'':= \begin{cases} 0 & \text{if } v_s \geq \tilde{v}_3'' \\ \frac{\tilde{v}_3'' - v_s}{\tilde{a}} - \left(\frac{a_s}{2\tilde{a}} + 1\right)t_1 & \text{if } v_s < \tilde{v}_3'' \end{cases}, \quad (32)$$

$$t''_6 := \begin{cases} 0 & \text{if } v_e \geq \bar{v}'_3 \\ \frac{\bar{v}'_3 - v_e}{\tilde{a}} + \left(\frac{a_e}{2\tilde{a}} - 1\right)t_1 & \text{if } v_e < \bar{v}'_3 \end{cases} . \quad (33)$$

Also this solution is not feasible because it does not fulfill neither the area, nor the velocity constraints (indeed, $v(t)$ can be equal to \tilde{v} inside $[0, t_e]$). Again, the acceleration constraint is certainly satisfied since $a_1(t_1) = \tilde{a}$ and $a_7(0) = -\tilde{a}$, while $v(t)$ assumes a shape that is similar to one of those that are shown in Fig. 3.

Step 4 - A feasible solution for *Problem 1* is found. In particular, \bar{v}_3 is posed equal to the minimum, positive-defined solution of the following equation

$$\sigma \bar{v}_3^2 + \eta \bar{v}_3 + \zeta = s_e , \quad (34)$$

where

$$\sigma = -\frac{t_6'' + t_2'' - t_6' - t_2'}{2(\bar{v}_3'' - \bar{v}_3')} , \quad (35)$$

$$\begin{aligned}\eta &= \frac{(t_2'' - t_2')(a_s t_1 + 2v_s + 2\bar{v}_3')}{4(\bar{v}_3'' - \bar{v}_3')} + t_e - 2t_1 - \frac{(t_2' + t_6')}{2} \\ &\quad - \frac{(t_6'' - t_6')(a_e t_1 - 2v_e - 2\bar{v}_3')}{4(\bar{v}_3'' - \bar{v}_2')} ,\end{aligned}\quad (36)$$

$$\zeta = \frac{a_s - a_e}{3} t_1^2 + \frac{a_s t_2' - a_e t_6'}{4} t_1 + (v_s + v_e) t_1 + \frac{v_s t_2' + v_e t_6'}{2} - \bar{v}_3' \frac{(2v_s + a_s t_1)(t_2'' - t_2') + (2v_e - a_e t_1)(t_6'' - t_6')}{4(\bar{v}_3' - \bar{v}_3)}. \quad (37)$$

The existence with certainty of such solution is proved in the Appendix section, where it is also shown that $\bar{v}_3 \in (\bar{v}'_3, \bar{v}''_3)$. The demonstration is based on the fulfillment of (5)–(7).

Traveling times t_2 and t_6 are successively selected as follows

$$t_2 := t'_2 + \frac{t''_2 - t'_2}{\bar{v}''_3 - \bar{v}'_3} (\bar{v}_3 - \bar{v}'_3), \quad (38)$$

$$t_6 \quad := \quad t'_6 + \frac{t''_6 - t'_6}{\bar{v}''_3 - \bar{v}'_3} (\bar{v}_3 - \bar{v}'_3) . \quad (39)$$

Despite the apparent complexity of (23)–(39), the procedure for the evaluation of the feasible solution is very efficient. Indeed, (23)–(39) are algebraic closed-form expressions that immediately return, when sequentially executed, a feasible solution for *Problem 1*.

Some final remarks can be useful to understand why the feasible solution has been obtained by means of the four steps approach. Smoothness represents one of the design requirements. In Appendix B, it will be shown that $v(t)$ is obtained by “averaging” the two solutions found at *Step 2* and *Step 3*. In this way, it is characterized by accelerations and velocities that are kept far from the given bounds. Moreover, the averaging effect applies also to the jerk, that is smaller for the final $v(t)$. Practically, the four steps approach returns solutions that, still being far from optimality, are sufficiently smooth to be directly used in a robotic context.

Such solutions are characterized by jerks that, still being finite, can potentially assume large values. For this reason, the final time-law is devised through a jerk minimization. To this purpose, the imposed restrictions on \mathbf{h} are first dropped, thus considering \mathbf{h} as composed by 11 independent parameters, then the acquired degrees of freedom are used to minimize the maximum jerk, by starting from feasible solution (23)–(39). Obviously, the optimization algorithm must preserve feasibility conditions (1)–(4). The adopted solver must possess two characteristics: It must be efficient, in order to be executed online, and it must return the final minimizer by passing through a sequence of feasible solutions. In this way, a feasible trajectory is constantly available and it can be used if convergence times are not compatible with the sampling rate. The optimization problem is nonlinear, so that the two requirements are very stringent.

An extension of a reliable and efficient algorithm, that was originally proposed in [13], has been used in next §V, while a more performing strategy can be found in [25]. Since the optimization algorithm is not the objective of this work, the interested reader can refer to that papers for details.

V. TEST CASES

The test problems proposed in the following are mainly intended to verify the approach effectiveness and its compatibility with an online implementation, so that particular attention has been devoted to the execution times.

The first problem concerns a critical situation, in which assigned planning data almost violate (6) and (7), so that the feasible zone is very narrow: Several commercial solvers were not able to converge to any feasible solution. The path length is $s_e = 11$, while traveling time is $t_e = 18$. The velocity and acceleration limits are respectively equal to $\tilde{v} = 0.7$, $\tilde{a} = 0.2$. The following boundary conditions are considered: $v_s = 0.01$, $v_e = 0.7$, $a_s = -0.2$, $a_e = 0.0$. The initial solution, found by means of (23)–(39), and the optimal one are compared in Fig. 7. Owing to the very critical planning conditions, the two solutions have similar shapes. Nevertheless, the optimal solution is characterized by a neatly smaller maximum jerk, as can be evinced from Table II.

The second example regards a less critical planning scenario, in which boundary conditions are well inside the feasible region. The path length is $s_e = 8$ while the traveling time is $t_e = 18$. The velocity and the acceleration limits are still equal to $\tilde{v} = 0.7$, $\tilde{a} = 0.2$, while boundary conditions are set equal to $v_s = 0.05$, $v_e = 0.4$, $a_s = -0.2$, $a_e = -0.2$. This time, the optimal solution is quite different from the initial one and it is characterized by a better performance index. In both cases, the velocity and the acceleration constraints are fulfilled, as can be evinced from Fig. 7. In the first example convergence is achieved in 2.74e-3 s (Intel Centrino 2, @2.53 GHz), while, in the second case, the solution is obtained in 3.22e-3 s. It is worth to point out that the computational burden is only due to the optimization process, while the initial solution is found by the four steps procedure in a negligible time.

Computational times are compatible with planning scenarios that require very frequent updates. It is important to establish the approach performances in case of early stops. To this purpose, an extended set of experiments has been executed. For each of them, the interpolating conditions have been randomly chosen among the following ranges: $s_e \in [10, 30]$, $t_e \in [10, 30]$, $\tilde{v} \in [0.4, 0.7]$, $\tilde{a} \in [0, 10]$, $v_s \in [0, \tilde{v}]$, $v_e \in [0, \tilde{v}]$, $a_s \in [-\tilde{a}, \tilde{a}]$, and $a_e \in [-\tilde{a}, \tilde{a}]$. Interpolating conditions that were not compatible with (5)–(7) have been discarded in advance, so that the algorithm proposed in §IV has always returned an initial feasible solution, that has been subsequently improved by means of the optimization strategy. Performances have been quantified through the difference, expressed in percentage, between the cost index that is obtained by early stopping the algorithm and the cost index that could have been obtained at the convergence. Each cell of Table II indicates the number of instances, over 100 runs, in which such difference is below the given thresholds. For example, if the algorithm is stopped after 5e-3 s, in the 92% of the runs the cost difference is below 1%. All solutions, even those concerning early interrupted instances, were feasible, since the optimization algorithm never abandons the feasible area.

VI. CONCLUSIONS

A feasibility issue regarding a constrained velocity planning problem has been analyzed and solved in the paper. In particular, necessary and sufficient conditions have been devised for the existence of

TABLE II
THE INITIAL GUESS \mathbf{h} AND THE FINAL SOLUTION \mathbf{h}^* FOR THE TWO TEST CASES

| t_1 | t_2 | t_3 | t_5 | t_6 | t_7 | \bar{v}_1 | \bar{v}_2 | \bar{v}_3 | \bar{v}_4 | \bar{v}_5 | j_{max} |
|----------------|--------|-------|--------|--------|-------|-------------|--------------------|-------------|-------------|-------------|-----------|
| First problem | | | | | | | | | | | |
| \mathbf{h} | 0.0333 | 3.30 | 0.0333 | 0.0333 | 0.132 | 0.0333 | 0.0100 | 0.670 | 0.673 | 0.673 | 0.676 |
| \mathbf{h}^* | 0.195 | 3.30 | 0.105 | 0.105 | 0.114 | 0.0873 | 9.98 ⁻³ | 0.670 | 0.681 | 0.666 | 0.676 |
| Second problem | | | | | | | | | | | |
| \mathbf{h} | 0.167 | 2.164 | 0.167 | 0.167 | 1.461 | 0.167 | 0.0493 | 0.463 | 0.478 | 0.478 | 0.475 |
| \mathbf{h}^* | 0.905 | 2.164 | 0.905 | 0.257 | 0.453 | 0.221 | 0.0336 | 0.395 | 0.478 | 0.478 | 0.473 |

TABLE III
CELLS REPORT THE NUMBER OF RUNS (OVER 100) IN WHICH THE COST INDEX AT THE STOP TIME DIFFERS FROM THE HOMOLOGOUS OF THE OPTIMAL SOLUTION FOR LESS THAN A GIVEN PERCENTAGE.

| stop time | 0.1% | 1% | 10% | 50% | 100% |
|-----------|------|----|-----|-----|------|
| 1e-3 s | 30 | 39 | 46 | 55 | 63 |
| 2e-3 s | 49 | 59 | 62 | 79 | 85 |
| 3e-3 s | 63 | 74 | 82 | 91 | 95 |
| 4e-3 s | 73 | 84 | 90 | 99 | 100 |
| 5e-3 s | 84 | 92 | 96 | 100 | 100 |

a velocity profile subject to velocity and acceleration constraints. If feasibility conditions are satisfied, a suitable solution is obtained by means of closed form expressions. Such solution can successively be improved through optimization algorithms that minimize the maximum longitudinal jerk. Reduced evaluation times have been verified, so that the approach can be suitably used in online planning schemes.

ACKNOWLEDGMENT

The author would like to thank Federico Canali and Marco Locatelli for the implementation of the validation tests.

REFERENCES

- [1] C.-S. Lin, P.-R. Chang, and J. Luh, "Formulation and optimization of cubic polynomial joint trajectories for industrial robots," *IEEE Trans. Automatic Control*, vol. AC-28, no. 12, pp. 1066–1074, 1983.
- [2] A. De Luca, L. Lanari, and G. Oriolo, "A sensitivity approach to optimal spline robot trajectories," *Automatica*, vol. 27, no. 3, pp. 535–539, May 1991.
- [3] C. Guarino Lo Bianco and A. Piazza, "A semi-infinite optimization approach to optimal trajectory planning of mechanical manipulators," in *Semi-Infinite Programming: Recent Advances*. Kluwer, 2001, ch. 13, pp. 271–297.
- [4] ———, "Minimum-time trajectory planning of mechanical manipulators under dynamic constraints," *Int. J. of Control*, vol. 75, no. 13, pp. 967–980, 2002.
- [5] S. Liu, "An on-line reference-trajectory generator for smooth motion of impulse-controlled industrial manipulators," in *Proc. of the seventh Int. Work. on Advanced Motion Control*, 2002, pp. 365–370.
- [6] S. Macfarlane and E. A. Croft, "Jerk-bounded manipulator trajectory planning: design for real-time applications," *IEEE Trans. on Robotics and Automation*, vol. 19, no. 1, pp. 42–52, 2003.
- [7] O. Gerelli and C. Guarino Lo Bianco, "A discrete-time filter for the on-line generation of trajectories with bounded velocity, acceleration, and jerk," in *IEEE Int. Conf. on Rob. and Autom., ICRA2010*, Anchorage, AK, May 2010, pp. 3989–3994.
- [8] R. Haschke, E. Weintrauer, and H. Ritter, "On-line planning of time-optimal, jerk-limited trajectories," in *Proc. of the IEEE/RSJ Int. Conf. on Intelligent Robots and Systems, IROS 08*, 2008, pp. 3248–3253.
- [9] X. Broquère, D. Sidobre, and I. Herrera-Aguilar, "Soft motion trajectory planner for service manipulator robot," in *Proc. of the 2008 IEEE/RSJ Int. Conf. on Intelligent Robots and Systems, IROS 08*, 2008, pp. 2808–2813.
- [10] T. Kröger and F. M. Wahl, "On-Line Trajectory Generation: Basic Concepts for Instantaneous Reactions to Unforeseen Events," *IEEE Trans. on Robotics*, vol. 26, no. 1, pp. 94–111, Feb. 2010.

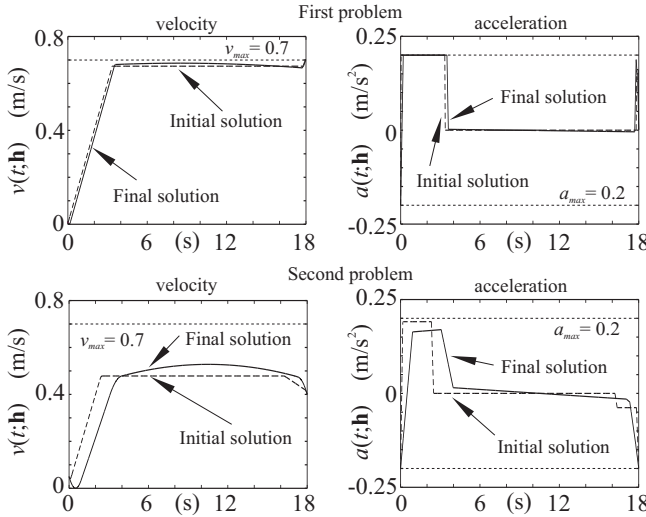


Fig. 7. A comparison between velocities and accelerations of the initial and final solutions.

- [11] C. Guarino Lo Bianco and O. Gerelli, "Online Trajectory Scaling for Manipulators Subject to High-Order Kinematic and Dynamic Constraints," *IEEE Trans. on Robotics*, vol. 27, no. 6, pp. 1144–1152, Dec. 2011.
- [12] J. Gyorfi and C.-H. Wu, "A Minimum-Jerk Speed-Planning Algorithm for Coordinated Planning and Control of Automated Assembly Manufacturing," *IEEE Trans. on Autom. Sci. and Eng.*, vol. 3, no. 4, pp. 454–462, Oct. 2006.
- [13] C. Guarino Lo Bianco and M. Romano, "Bounded Velocity Planning for Autonomous Vehicles," in *2005 IEEE/RSJ Int. Conf. on Intelligent Robots and Systems, IROS'05*, Edmonton, Canada, August 2005, pp. 4068–4073.
- [14] A. Gasparetto and V. Zanotto, "A technique of time-jerk optimal planning of robot trajectories," *Robotics and Computer-Integrated Manufacturing*, vol. 24, pp. 415–426, 2008.
- [15] K. Kyriakopoulos and G. Saridis, "Minimum jerk path generation," in *IEEE Int. Conf. on Rob. and Autom., ICRA'88*, apr 1988, pp. 364–369 vol.1.
- [16] A. Piazzoli and A. Valsioli, "Global minimum-jerk trajectory planning of robot manipulators," *IEEE Trans. on Ind. Electr.*, vol. 47, no. 1, pp. 140–149, feb 2000.
- [17] F. Amirabdollahian, R. Loureiro, and W. Harwin, "Minimum jerk trajectory control for rehabilitation and haptic applications," in *Proc. of the IEEE Int. Conf. on Rob. and Autom., ICRA'02*, vol. 4, 2002, pp. 3380–3385.
- [18] P. Huang, K. Chen, J. Yuan, and Y. Xu, "Motion Trajectory Planning of Space Manipulator for Joint Jerk Minimization," in *Int. Conf. on Mechat. and Autom., ICMA 2007*, aug. 2007, pp. 3543–3548.
- [19] C. Guarino Lo Bianco, "Optimal velocity planning for autonomous vehicles under kinematic constraints," in *8th Int. IFAC Symp. on Robot Control, SYROCO 2006*, Bologna, Italy, Sept. 2006.
- [20] —, "Kinematically constrained smooth real-time velocity planning for robotics applications," in *IEEE Int. Conf. on Contr. and Autom., ICCA 2009*, dec. 2009, pp. 373–378.
- [21] C. Guarino Lo Bianco, A. Piazzoli, and M. Romano, "Smooth motion generation for unicycle mobile robots via dynamic path inversion," *IEEE Trans. on Robotics*, vol. 20, no. 5, pp. 884–891, Oct. 2004.
- [22] K. Kant and S. Zucker, "Toward efficient trajectory planning: The path-velocity decomposition," *Int. J. Robot. Res.*, vol. 5, no. 3, pp. 72–89, 1986.
- [23] A. Piazzoli, C. Guarino Lo Bianco, and M. Romano, " η^3 -splines for the smooth path generation of wheeled mobile robots," *IEEE Trans. on Robotics*, vol. 23, NO. 5, pp. 1089–1095, 2007.
- [24] C. Guarino Lo Bianco and M. Romano, "Optimal velocity planning for autonomous vehicles considering curvature constraints," in *Proc. of the IEEE Int. Conf. on Rob. and Autom., ICRA2007*, april 2007, pp. 2706–2711.
- [25] F. Canali, C. Guarino Lo Bianco, and M. Locatelli, "Minimum-jerk online planning by a mathematical programming approach," *Engineering Optimization*, To appear.

APPENDIX

The algorithm that has been proposed in §IV returns a feasible solution for *Problem 1* every time conditions (5)–(7) are satisfied. In order to prove this assertion, let us draw some preliminary considerations. The velocity profile that is shown Fig. 6 has the following characteristics:

- In the second, fourth, and sixth time intervals, $v(t)$ is linear, so that $a(t)$ is constant. Moreover, in the fourth time interval $v(t)$ is constant and $a(t) = 0$;
- In the first, third, fifth, and seventh time intervals, $v(t)$ is parabolic;
- Time intervals are chosen such that $t_1 = t_3 = t_5 = t_7$;

Several conclusions can be drawn from the above mentioned characteristics:

- The acceleration constraint can only be violated in the second and in the sixth time intervals.
- The velocity function can only admit maxima or minima along the parabolic segments. Nevertheless, in the third interval, because of the acceleration continuity, such maximum (or minimum) coincides with the segment end, i.e., it is equal to $v_3(t_3) = \bar{v}_3$, while in the fifth interval it coincides with the segment beginning, i.e., $v_5(0) = \bar{v}_3$: If \bar{v}_3 is feasible, the velocity constraint cannot be violated in such intervals, so that the first and the seventh segments are the sole candidates for the velocity constraint violation.

The four steps algorithm generates feasible solutions for generic interpolating conditions. However, for the sake of brevity, only the feasibility of the most general case, characterized by $v_s \in (0, \bar{v})$ and $v_e \in (0, \bar{v})$, will be discussed in the following. The proof for specific cases, where initial and final velocities lie on the borders of the feasible area, i.e., $v_s = 0$ or $v_s = \bar{v}$ or $v_e = 0$ or $v_e = \bar{v}$, is left to the reader and can be devised according to the same procedure.

A. The velocity constraint

It was early stated that, if \bar{v}_3 is feasible, the velocity constraint can only be violated in the first and in the last time intervals. This can happen if $v(t)$ has a minimum or a maximum inside those intervals.

Let us consider the first interval. $v_1(t)$ is a parabola, so that the velocity profile admits a minimum or a maximum only if a_s and \bar{a}_1 have opposite signs. This implies that, for any other possible combination of a_s and \bar{a}_1 , including those where $a_s = 0$ or $\bar{a}_1 = 0$ ¹, the velocity constraint cannot be violated. Let us consider the following proposition:

Proposition 2: If a_s and \bar{a}_1 have opposite sign and t_1 is selected as follows

$$t_1 \leq \begin{cases} -\frac{2v_s}{a_s} & \text{if } a_s < 0 \text{ and } \bar{a}_1 > 0 \\ \frac{2(\bar{v}-v_s)}{a_s} & \text{if } a_s > 0 \text{ and } \bar{a}_1 < 0 \end{cases}, \quad (40)$$

condition (2) is fulfilled with certainty in the first time interval.

Proof - The acceleration at the end of the first time interval, is given by

$$a_1(t_1) = \bar{a}_1 = a_s + \frac{2(\bar{v}_3 - v_s) - (2t_2 + 3t_1)a_s}{2(t_2 + t_1)}. \quad (41)$$

Equation (41) can be solved for t_2 , thus leading to

$$t_2 = \frac{2(\bar{v}_3 - v_s) - (a_s + 2\bar{a}_1)t_1}{2\bar{a}_1}. \quad (42)$$

¹If $a_s = 0$ then $\max_t\{v_1(t)\} = v_1(0) = v_s \in [0, \bar{v}]$, while if $\bar{a}_1 = 0$ it is easily possible to prove that, owing to the shape of the simplified solution and to the imposed continuity conditions, $\max_t\{v_1(t)\} = v_1(t_1) = \bar{v}_1 = \bar{v}_2 = \bar{v}_3$.

In turn, (42) makes it possible to write $v_1(t)$ as follows

$$v_1(t) = v_s + a_s t + \frac{\bar{a}_1 - a_s}{2t_1} t^2. \quad (43)$$

The maximum (or minimum) of (43) is equal to

$$v_1(t_p) = v_s - \frac{a_s^2 t_1}{2(\bar{a}_1 - a_s)}. \quad (44)$$

If $a_s < 0$ and $\bar{a}_1 > 0$ the velocity has a minimum inside the first time interval and $v_1(t_p)$ could become negative or equal to zero, thus violating (2). In order to avoid this situation, it is sufficient to select t_1 such that $v_1(t_p) > 0$. From (44) it is possible to infer that such condition is satisfied if the following inequality holds

$$t_1 < 2v_s \frac{\bar{a}_1 - a_s}{a_s^2}. \quad (45)$$

This result is automatically achieved if (40) is satisfied. Indeed, by also taking into account that $\bar{a}_1 > 0$, it is possible to write

$$2v_s \frac{\bar{a}_1 - a_s}{a_s^2} > -2v_s \frac{a_s}{a_s^2} = -\frac{2v_s}{a_s} \geq t_1. \quad (46)$$

Similarly, if $a_s > 0$ and $\bar{a}_1 < 0$ the velocity has a maximum inside the first interval and $v_1(t_p)$ could become greater than \tilde{v} . This situation is avoided by selecting t_1 such to guarantee that $v_1(t_p) \leq \tilde{v}$. From (44) it is possible to infer that feasibility is ensured by imposing

$$t_1 \leq -\frac{2(\bar{a}_1 - a_s)(\tilde{v} - v_s)}{a_s^2}. \quad (47)$$

This condition is strictly satisfied for any $\bar{a}_1 < 0$ if (40) holds. Indeed

$$-\frac{2(\bar{a}_1 - a_s)(\tilde{v} - v_s)}{a_s^2} > \frac{2a_s(\tilde{v} - v_s)}{a_s^2} = \frac{2(\tilde{v} - v_s)}{a_s} \geq t_1. \quad (48)$$

■

With analogous arguments it is possible to prove that the velocity constraint is also satisfied in the last time interval by imposing (remember that $t_7 = t_1$)

$$t_1 \leq \begin{cases} \frac{2v_e}{a_e} & \text{if } a_e > 0 \text{ and } \bar{a}_6 < 0 \\ \frac{2(\tilde{v}_3 - \tilde{v})}{a_e} & \text{if } a_e < 0 \text{ and } \bar{a}_6 > 0 \end{cases} \quad (49)$$

Remark 1: Because of (40) and (49), the velocity constraint is satisfied with certainty, for any $t_2, t_6 \geq 0$ and $\tilde{v}_3 \in (0, \tilde{v})$, provided that a sufficiently small value of t_1 is selected.

Proposition 3: The velocity constraint is satisfied or, equivalently, (40) and (49) are fulfilled, if t_1 is selected according to (23)–(25).

Proof - Still considering the general case, i.e., $v_s \in (0, \tilde{v})$ and $v_e \in (0, \tilde{v})$, let us focus the attention on the first time interval and suppose that $\bar{a}_1 < 0$, while $a_s > 0$: The upper velocity bound can be violated. Two possible situations can be prefigured depending on $v_s + v_e + \tilde{a}t_e$. In particular, if $v_s + v_e + \tilde{a}t_e > 2\tilde{v}$, then, due to (24), it is possible to write

$$t_1 \leq \frac{2(\tilde{v} - v_s)}{2\tilde{a} + a_s} < \frac{2(\tilde{v} - v_s)}{a_s},$$

and to conclude that the velocity constraint is fulfilled because of (40). Otherwise, if $v_s + v_e + \tilde{a}t_e \leq 2\tilde{v}$, then, due to (25), the velocity constraint is satisfied since the following inequality holds

$$t_1 \leq \frac{2(v_e - v_s + t_e \tilde{a})}{10\tilde{a} + a_e + a_s} < \frac{v_e - v_s + 2\tilde{v} - v_s - v_e}{\tilde{a}} \leq \frac{2(\tilde{v} - v_s)}{a_s}.$$

In the same way, if $a_s < 0$ and $\bar{a}_1 > 0$, the velocity could become negative. Again, two scenarios can be considered depending on the sign of $v_s + v_e - \tilde{a}t_e$. If $v_s + v_e - \tilde{a}t_e < 0$, from (23) it descends that

$$t_1 \leq \frac{2v_s}{2\tilde{a} - a_s} < -\frac{2v_s}{a_s},$$

i.e., (40) is satisfied. If $v_s + v_e - \tilde{a}t_e \geq 0$, then (40) is fulfilled since from (25) we can infer that

$$t_1 \leq \frac{2(v_s - v_e + t_e \tilde{a})}{10\tilde{a} - a_e - a_s} < \frac{2(v_s - v_e + v_s + v_e)}{2\tilde{a}} \leq \frac{4v_s}{-2a_s} = -\frac{2v_s}{a_s}.$$

By means of similar arguments, it is possible to demonstrate that (23)–(25) also guarantee the velocity boundedness in the last time interval. Demonstration is omitted for brevity. ■

B. Feasibility of the four steps solution

As shown in subsection A, it is always possible to fulfill the velocity constraint in the first and in the last time intervals by choosing a sufficiently small t_1 . Relations (5)–(7) are essential in order to prove the feasibility of the four steps solution.

Let us indicate by S the area of $v(t)$, i.e., the path length corresponding to $v(t)$. The four steps approach requires the evaluation of three different velocity profiles. The first two are unfeasible. In particular, they do not strictly satisfy the velocity and the area constraints. The final solution is feasible and it is found by combining the first two.

Solution found at Step 2 ($S < s_e$) - The velocity function, that is obtained by means of (28)–(30), is unfeasible. Indeed, it will be shown in the following that, nevertheless its traveling time is equal to t_e and it fulfills requirements (3) and (4), its area is $S < s_e$, i.e., (1) is not satisfied, and it also violates (2), since $v(t)$ can be equal to zero for $t \in [0, t_e]$.

If condition $t_i \geq 0$ applies for $i = 1, 2, \dots, 7$, then the traveling time requirement is fulfilled owing to (21). Times $t_1 = t_3 = t_5 = t_7$ are selected according to (23)–(27), thus they are certainly positive, while the sign of t'_2 , t'_4 , and t'_6 , depends on the planning data. Remember that, for conciseness, it has been assumed that $v_s \in (0, \tilde{v})$ and $v_e \in (0, \tilde{v})$. Thus, according to (28), two different solutions are possible depending on the sign of $v_s + v_e - \tilde{a}t_e$. Let us first hypothesize that

$$v_s + v_e - \tilde{a}t_e < 0. \quad (50)$$

$\tilde{v}_3' = 0$ due to (28): According to *Proposition 3*, the velocity constraint is verified everywhere, apart from the fourth time interval.

Let us prove the positivity of t'_2 . Due to (29) and since $v_s > \tilde{v}_3' = 0$, it is possible to infer that $t'_2 = \frac{v_s}{\tilde{a}} + \left(\frac{a_s}{2\tilde{a}} - 1\right)t_1$. Term $\left(\frac{a_s}{2\tilde{a}} - 1\right)$ is strictly negative, thus because of (23), the following inequality holds

$$t'_2 \geq \frac{v_s}{\tilde{a}} + \left(\frac{a_s - 2\tilde{a}}{2\tilde{a}}\right) \frac{2v_s}{2\tilde{a} - a_s} = 0.$$

In the same way, from (30) it is possible to deduce, since $\left(\frac{a_e}{2\tilde{a}} + 1\right)$ is positive and (23) holds, that

$$t'_6 = \frac{v_e}{\tilde{a}} - \left(\frac{a_e}{2\tilde{a}} + 1\right)t_1 \geq \frac{v_e}{\tilde{a}} - \left(\frac{a_e + 2\tilde{a}}{2\tilde{a}}\right) \frac{2v_e}{2\tilde{a} + a_e} = 0.$$

The sign of t'_4 can be verified by substituting (29) and (30) into (21). After a few algebraic manipulations, it is possible to write

$$t'_4 = \frac{a_e - a_s - 4\tilde{a}}{2\tilde{a}} t_1 - \frac{v_s + v_e - t_e \tilde{a}}{\tilde{a}}.$$

Term $\frac{a_e - a_s - 4\tilde{a}}{2\tilde{a}}$ is clearly negative, so that, owing to (23) and (50), the following inequality is satisfied

$$t'_4 \geq \frac{a_e - a_s - 4\tilde{a}}{2\tilde{a}} 2 \frac{v_s + v_e - t_e \tilde{a}}{a_e - a_s - 4\tilde{a}} - \frac{v_s + v_e - t_e \tilde{a}}{\tilde{a}} = 0.$$

The fulfillment of the acceleration constraint is straightforward owing to the shape of $a(t)$. From Fig. 6, it is evident that (3) can only be violated in the second and in the sixth time intervals. However, it is easy to verify, with few algebraic manipulations, that (28)–(30) always generate a profile in which $a_1(t_1) = a_2(0) = -\tilde{a}$ and $a_6(t_6) = a_7(0) = \tilde{a}$.

It is further necessary to check if condition $S < s_e$ holds. Once \bar{v}_3, t_2 , and t_6 have been assigned according to (28)–(30), S can be posed into the following form

$$S = \alpha t_1^2 + \beta t_1 + \gamma, \quad (51)$$

where α, β , and γ are appropriate coefficients. Equation (51) can also be written as follows

$$S = \underbrace{\alpha t_1^2 + \beta t_1}_{\xi} + \underbrace{\gamma - s_e + s_e}_{\delta}. \quad (52)$$

Coefficients α, β , and δ are those reported in the fourth row of Tab. I. Evidently $\delta < 0$ owing to (7), so that, by choosing a sufficiently small t_1 , it is certainly possible to impose $\xi + \delta < 0$ and to achieve, as desired, $S = \xi + \delta + s_e < s_e$. An upper bound for t_1 can be found by selecting the minimum real, positive solution \tilde{t} (if any) of equation $\alpha \tilde{t}^2 + \beta \tilde{t} + \delta = 0$ and by imposing $t_1 < \tilde{t}$: This inequality is fulfilled because of (26) and, consequently, $S < s_e$. If $\alpha \tilde{t}^2 + \beta \tilde{t} + \delta = 0$ admits no real positive solutions then, evidently, condition $\xi + \delta < 0$ is always satisfied independently from t_1 , thus t_1 is only bounded by the other inequalities of list (23)–(27).

Previous considerations apply for $v_s + v_e - \tilde{a}t_e < 0$. In the following it is proved that similar considerations are also valid when

$$v_s + v_e - \tilde{a}t_e \geq 0. \quad (53)$$

According to (28), \bar{v}'_3 is given by

$$\bar{v}'_3 = \frac{6\tilde{a} + a_s - a_e}{4} t_1 + \frac{v_s + v_e - t_e \tilde{a}}{2}. \quad (54)$$

Now, $\bar{v}'_3 > 0$ with certainty. Thus, according to (29), t'_2 can assume two different values: $t'_2 = 0$ or

$$t'_2 = -\frac{10\tilde{a} - a_s - a_e}{4\tilde{a}} t_1 + \frac{v_s - v_e + t_e \tilde{a}}{2\tilde{a}}.$$

In the second case, term $-\frac{10\tilde{a} - a_s - a_e}{4\tilde{a}}$ is clearly negative, while $\frac{v_s - v_e + t_e \tilde{a}}{2\tilde{a}} \geq 0$ owing to (5). Bearing in mind (25), it is possible to write

$$t'_2 \geq -\frac{10\tilde{a} - a_s - a_e}{4\tilde{a}} 2 \frac{v_s - v_e + t_e \tilde{a}}{10\tilde{a} - a_s - a_e} + \frac{v_s - v_e + t_e \tilde{a}}{2\tilde{a}} = 0,$$

and conclude that, as required, $t'_2 \geq 0$. Similarly for t'_6 we have $t'_6 = 0$ or

$$t'_6 = -\frac{10\tilde{a} + a_s + a_e}{4\tilde{a}} t_1 + \frac{v_e - v_s + t_e \tilde{a}}{2\tilde{a}}.$$

Being $-\frac{10\tilde{a} + a_s + a_e}{4\tilde{a}} < 0$, while, owing to (5), $\frac{v_e - v_s + t_e \tilde{a}}{2\tilde{a}} \geq 0$, due to (25) it is possible to write

$$t'_6 \geq -\frac{10\tilde{a} + a_s + a_e}{4\tilde{a}} 2 \frac{v_e - v_s + t_e \tilde{a}}{10\tilde{a} + a_e + a_s} + \frac{v_e - v_s + t_e \tilde{a}}{2\tilde{a}} = 0.$$

Finally, by evaluating t'_4 according to (21), the following result is immediately achieved

$$t'_4 = t_1 > 0.$$

By means of few algebraic manipulations, it is newly possible to prove that $a_1(t_1) = -\tilde{a}$ and $a_7(0) = \tilde{a}$, thus (3) is verified

The area of $v(t)$ can still be expressed into one of the two forms (51) or (52), where coefficients α, β , and γ are those reported in the fifth row of Tab. I. Like in the previous case, δ_i is negative owing to (7), so that inequality (26) guarantees that $S < s_e$.

Solution found at Step 3 ($S > s_e$) - The solution that is found at Step 3 shows similar characteristics, but its area is $S > s_e$. The demonstration, that is based on the use of (5) and (6), is omitted for the sake of conciseness, but it mimics the procedure followed for the solution that was found at Step 2. It is worth to point out that the new

solution is characterized by the following accelerations: $a_1(t_1) = \tilde{a}$ and $a_6(t_6) = -\tilde{a}$.

Solution found at Step 4 ($S = s_e$) - The final feasible solution is obtained by selecting t_1 according to (23)–(27), $\bar{v}_3 \in (\bar{v}'_3, \bar{v}''_3)$ is found by solving (34), while traveling times $t_2(\bar{v}_3)$ and $t_6(\bar{v}_3)$ are evaluated according to (38) and (39).

Equation (34), that imposes $S = s_e$, admits with certainty at least one solution $\bar{v}_3 \in (\bar{v}'_3, \bar{v}''_3)$. Indeed, if traveling times t_2, t_6 and t_4 are assigned according to (38), (39), and (21), the total area of $v(t)$ can be expressed as follows

$$S = \sigma \bar{v}_3^2 + \eta \bar{v}_3 + \zeta, \quad (55)$$

where σ, η , and ζ are defined according to (35)–(37). By assuming $\bar{v}_3 = \bar{v}'_3$, (38) and (39) return $t_2 = t'_2$ and $t_6 = t'_6$, i.e., the velocity profile is the same found at Step 2 and its area is $S < s_e$. Conversely, if $\bar{v}_3 = \bar{v}''_3$, the velocity profile is the same found at Step 3, so that $S > s_e$. Due to the continuity of (55), there exists with certainty a value of $\bar{v}_3 \in (\bar{v}'_3, \bar{v}''_3)$ such that $S = s_e$. Such value can be found by solving (34) and it is feasible only if (2) and (3) are satisfied, all traveling times are positive and their sum is equal to t_e .

Traveling times $t_1 = t_3 = t_5 = t_7$, being chosen according to (23)–(27), are certainly positive. Moreover, it has been proved in Appendix A that (23)–(27) guarantee the feasibility with respect to the velocity constraint for any feasible value of \bar{v}_3 : The chosen value of \bar{v}_3 is evidently feasible being $\bar{v}_3 \in (\bar{v}'_3, \bar{v}''_3)$. t_2 and t_6 are positive since they are evaluated according to (38) and (39): They linearly depend on \bar{v}_3 and are evidently bounded between t'_2 and t''_2 and between t'_6 and t''_6 , i.e., $t_2 \in (t'_2, t''_2)$ and $t_6 \in (t'_6, t''_6)$. t_4 is evaluated according to (21) so that, evidently, the traveling time requirement is satisfied provided that $t_4 > 0$. Solutions that were found at Step 2 and Step 3 fulfill (21) and, consequently, it is possible to write $t'_4 = t_e - 4t_1 - t'_2 - t'_6$ and $t''_4 = t_e - 4t_1 - t''_2 - t''_6$, and, in turn,

$$-(t''_4 - t'_4) = (t''_2 - t'_2) + (t''_6 - t'_6). \quad (56)$$

By substituting (38) and (39) in (21), and by also considering (56), after few algebraic manipulations, it is possible to write

$$t_4 = t'_4 + \frac{(t''_4 - t'_4)}{\bar{v}''_3 - \bar{v}'_3} (\bar{v}_3 - \bar{v}'_3),$$

i.e., t_4 linearly depends on \bar{v}_3 and it lies in the positive open interval between t'_4 and t''_4 , i.e., $t_4 \in (t'_4, t''_4)$.

Finally, the fulfillment of (3) can be easily checked. As usual, (3) can only be violated at the end of the first or at the beginning of the last time intervals. Let us consider the first possibility, keeping in mind that the second one can be handled by means of similar reasonings. By virtue of (38), (41) can be posed, after several algebraic manipulations, into the following form

$$a_1(t_1) = \frac{\xi_1 + \xi_2 \bar{v}_3}{\xi_3 + \xi_4 \bar{v}_3}, \quad (57)$$

where $\xi_i, i = 1, 2, 3, 4$ are given constants that only depend on the interpolating conditions. Practically, $a_1(t_1)$ hyperbolically depends on \bar{v}_3 and, consequently, is monotonic. Moreover, the vertical asymptote of $a_1(t_1)$ lies outside interval $[\bar{v}'_3, \bar{v}''_3]$ since its denominator, being given by $2(t_1 + t_2)$, can never be equal to zero. Due to Step 2 and Step 3, when $\bar{v}_3 = \bar{v}'_3$ we have $t_2 = t'_2$ and $a_1(t_1) = -\tilde{a}$, while when $\bar{v}_3 = \bar{v}''_3$ we have: $t_2 = t''_2$ and $a_1(t_1) = \tilde{a}$. Owing to the monotonicity of (57), it is possible to conclude that $a_1(t_1) \in (-\tilde{a}, \tilde{a}), \forall \bar{v}_3 \in (\bar{v}'_3, \bar{v}''_3)$.